JOURNAL OF GUIDANCE, CONTROL, AND DYNAMICS
Vol. 22, No. 5, September–October 1999

Optimal Aeroassisted Orbital Interception

Kazuhiro Horie* and Bruce A. Conway†
University of Illinois at Urbana–Champaign, Urbana, Illinois 61801

Optimal trajectories are found for the interception of a target in circular, low Earth orbit, by a vehicle that is initially in a higher orbit. The interceptor vehicle can use both conventional rocket propulsion and, if optimal or necessary, aerodynamic forces to change its orbit. The problem is solved using a direct method, collocation with nonlinear programming, in which the continuous optimal control problem is converted into a discrete problem. Both minimum-time and minimum-fuel trajectories are found. The sensitivity of the optimal trajectories to atmospheric heating-rate constraints is determined. An interesting result is that some minimum-time trajectories enter the atmosphere and use aerodynamic forces for orbit change even when there is sufficient propellant available to accomplish the interception ballistically.

Introduction

IN this work, optimal trajectories for an aeroassisted orbital transfer vehicle (AOTV) are found. An AOTV is an aerospace vehicle that has the capability of changing its orbit using conventional rocket propulsion in space or using aerodynamic forces during passage through an atmosphere. After using the aerodynamic force and getting the necessary velocity vector change, the AOTV escapes from the Earth's atmosphere and transfers to a new orbit. Thus, an AOTV can modify its orbit during atmospheric flight without using fuel by changing its total energy and its momentum via aerodynamic lift and drag. Aeroassisted orbital transfer (AOT) can reduce the total fuel necessary to accomplish a mission or to reach an orbit impossible to reach using only propulsive maneuvers with given fuel. However, the advantages of AOT come with certain features that complicate the optimal control problem: The vehicle is subject to intense heating that must not exceed a given limit, the system governing equations are more complex than those for space flight alone, and additional controls must be employed for atmospheric flight.

The optimal trajectories are found here using numerical optimization. Numerical trajectory optimization methods are generally divided into two categories. One is the indirect method, which yields necessary conditions that constitute a two-point boundary-value problem (TPBVP). In the case of constraints on the controls and states in a problem, it is necessary to formulate differential equations on the basis of the Pontryagin principle and multiboundary conditions resulting from the state constraints.[1] It is usually difficult to solve these TPBVPs numerically because of their nonlinearity. Another category of solution methods consists of the direct methods in which the optimal control problem is converted into a parameter optimization problem. There are many techniques available for this transformation[2–5]; a direct method termed direct collocation with nonlinear programming (DCNLP) has been applied successfully to many trajectory optimization problems and is used in this work. It will be briefly described in a later section.

The AOTV trajectory optimization problem has been studied for decades. With regard to recent research, in 1987, Miele et al.[6] published solutions for optimal noncoplanar orbit transfer using a combination of impulsive maneuvers in space and aerodynamic maneuvers in the atmosphere. A 1996 paper by Miele[7] examines both AOTV trajectory optimization and guidance. It also contains an extensive bibliography documenting many years of research by the author, his colleagues, and others.

Medepalli and Vinh[8] focus on the extension of transfer range in their latest study in this area. Accordingly, they selected the terminal inclination change as the cost function and all other terminal state variables as the terminal conditions. They assumed an aerocruising AOTV, which uses low thrust to cancel the drag through atmospheric flight. The thrust balanced to the drag for aerocruise was dealt with as a constraint and was directly included in the governing equations. To solve their problem, a shooting method, a kind of indirect method, was applied.

Naidu[9] published his AOTV studies in 1994. In his research, two different types of AOTV trajectory optimization, aeroglide and aerocruise, were solved by using fuel consumption as a cost function. As in Refs. 6 and 7, Naidu did not use the state variable constraint and did use a circular orbit injection as a terminal condition. He used the multiple shooting method for his numerical solutions.

Seywald[10] published results for AOTV trajectory optimization in 1996. He solved for the optimal orbit to maximize the final velocity for given final altitude and orbit inclination under heating constraints, a type of state variable constraint. The Pontryagin principle was used for the formulation of the optimal control problem, and a multiboundary condition problem was constructed. He used a shooting method in combination with (and assisted with) analysis concerning the nature of the solution, which allowed him, for example, to determine a priori the optimal switching structure.

Lee and Hull[11] reported solutions to maximize AOTV orbit plane change. Their study was conducted to compare the capability of aerogliding AOTV and aerocruising AOTV for orbit plane change. For this purpose, the terminal altitude was fixed. They solved for optimal trajectories with a heating rate constraint, using a direct method.

Through reviews of past research, it appears that the use of the DCNLP solution method should yield great advantages for AOTV trajectory optimization. To determine realistic optimal trajectories, state variable constraints such as heating-rate constraints must be considered. However, this may be problematic. Miele et al.,[6] Miele,[7] and Naidu[9] avoided using state variable constraints. Although Medepalli and Vinh[8] and Seywald[10] used the state variable constraint, they needed a complicated interpretation of this constraint so that the optimal control problem included this constraint. All of these studies used the indirect method. The use of the direct method can include the state variable constraint without special treatment. Lee and Hull[11] used this approach in their research. The DCNLP method has also been shown to yield advantages over indirect methods in terms of problem size and robustness, which are likely to apply to the solution of this problem as well.

In this work, the DCNLP method will be applied to the solution of an optimal aeroassisted interception problem with and without heating-rate constraints, in which a target in low Earth orbit is intercepted by an AOTV originally in a higher orbit. The AOTV deorbits

Received 5 August 1998; revision received 1 April 1999; accepted for publication 5 April 1999.

*Graduate Research Assistant, Department of Aeronautical and Astronautical Engineering.

†Professor, Department of Aeronautical and Astronautical Engineering; bconway@uiuc.edu. Associate Fellow AIAA.

from an initial circular orbit using an impulse whose magnitude and direction is chosen optimally. Optimal trajectories will be found for both minimum-time and minimum-fuel cases.

However, before proceeding to this solution, a simpler but qualitatively similar problem, i.e., an optimal orbit transfer problem using an AOTV, with and without heating-rate constraints, will be solved so that the results using DCNLP may be compared with an extant solution. The comparison will confirm the presupposed advantages of using the DCNLP method described in the preceding paragraphs.

Equations of Motion

The motion of the spacecraft, from deorbiting to interception, is described using the same equations of motion in space and in the atmosphere. A coordinate frame is fixed in space for both space and atmospheric flight. As a stationary atmosphere is assumed, velocity relative to space is the same as velocity relative to the atmosphere. Therefore, aerodynamic force as a function of velocity relative to the atmosphere is simply expressed in a space-fixed frame. It is also advantageous that it is not necessary to convert from an Earth-fixed frame to a space-fixed frame. All modeling to express AOT interception is done on this space-fixed frame. Forces exerted on the AOTV are aerodynamic lift and drag and the force of gravity. Therefore, polar coordinates are used to locate the AOTV because of convenience in expressing the gravity force. The AOTV stationary orbit plane is set as the latitude reference plane. Radius r is defined as distance from the center of the Earth. Latitude ϕ is measured as the angle between the radius line and the projection of the radius line to the latitude reference plane. Longitude θ is measured from the deorbiting point along the latitude reference plane.

It is necessary for the AOTV to use thrust to deorbit from its initial stationary circular orbit. The deorbiting thrust is assumed to be applied impulsively; the impulsive thrust assumption on the basis of Prussing and Conway[12] can be applied to this model.

Let the velocity vector on the initial AOTV stationary circular orbit be $\boldsymbol{v}_{s0}$ and the velocity vector immediately after the deorbiting impulse be $\boldsymbol{v}_0$. The difference between these two vectors is the impulsive, initial velocity change vector $\mathrm{d}\boldsymbol{v}$. Its maximum magnitude $\mathrm{d}v_{\max}$ is determined by the fuel limitation. A relation among these velocity vectors is derived from the cosine law. When the angle between $\boldsymbol{v}_{s0}$ and $\boldsymbol{v}_0$ is defined as δ, the relation is expressed as

$$\mathrm{d}v_{\max}^2 \geq \mathrm{d}v^2 = v_{s0}^2 + v_0^2 - 2v_{s0} \cdot v_0 \cdot \cos\delta \tag{1}$$

where $\mathrm{d}v$, v_{s0}, and v_0 are the magnitudes of $\mathrm{d}\boldsymbol{v}$, $\boldsymbol{v}_{s0}$, and $\boldsymbol{v}_0$, respectively.

Flight-path angle and heading angle are zero on the stationary circular orbit. When flight-path angle and heading angle of the AOTV immediately after deorbiting are set to γ_0 and ψ_0, respectively, δ is related to γ_0 and ψ_0 by

$$\cos\delta = \cos\gamma_0 \cdot \cos\psi_0 \tag{2}$$

Therefore, the relationship among velocity, flight-path angle, and heading angle immediately after deorbiting is described by

$$\mathrm{d}v_{\max}^2 \geq \mathrm{d}v^2 = v_{s0}^2 + v_0^2 - 2v_{s0} \cdot v_0 \cdot \cos\gamma_0 \cdot \cos\psi_0 \tag{3}$$

Velocity, flight-path angle, and heading angle resulting from Eq. (3) are used as initial conditions in the equations of motion.

Vinh et al.[13] introduced a set of equations of motion for nonthrusting entry to a nonrotating planetary atmosphere. In this study, essentially the same equations of motion are used, but altitude from the Earth's surface is used as a state variable instead of radius from the center of the Earth because if radius is used as a state variable, its change relative to the Earth radius is very small. The modified equations of motion are

$$\dot{v} = -\frac{D}{m} - \frac{\mu}{(r_e + h)^2}\sin\gamma \tag{4}$$

$$\dot{\gamma} = \frac{L\cos\sigma}{mv} + \left[\frac{v}{(r_e + h)} - \frac{\mu}{v(r_e + h)^2}\right]\cos\gamma \tag{5}$$

$$\dot{\psi} = \frac{L\sin\sigma}{mv\cos\gamma} - \frac{v}{(r_e + h)}\cos\gamma \cdot \cos\psi \cdot \tan\phi \tag{6}$$

$$\dot{h} = v\sin\gamma \tag{7}$$

$$\dot{\theta} = \frac{v\cos\gamma \cdot \cos\psi}{(r_e + h)\cos\phi} \tag{8}$$

$$\dot{\phi} = \frac{v\cos\gamma \cdot \sin\psi}{(r_e + h)} \tag{9}$$

where r_e is the radius of the Earth, μ is the gravitational parameter of the Earth, and m is the mass of the spacecraft.

The set of equations includes six state variables, velocity v, flight-path angle γ, heading angle ψ, altitude h, longitude θ, and latitude ϕ, and two control variables, lift coefficient C_L and bank angle σ. As no thrust is used, the vehicle mass is constant.

Aerodynamic forces in Eqs. (4–6), which consist of lift force and drag force, are given by

$$L = \tfrac{1}{2}\rho v^2 S C_L \tag{10}$$

$$D = \tfrac{1}{2}\rho v^2 S C_D \tag{11}$$

where S is the cross-sectional area of the spacecraft presented to the flow.

The drag coefficient is modeled using the lift coefficient C_L and minimum drag coefficient C_{D0} as[14]

$$C_D = C_{D0} + K C_L^2 \tag{12}$$

Atmospheric density is assumed to change exponentially as

$$\rho = \rho_s e^{-h/\beta} \tag{13}$$

where β is the atmospheric scale height.

Equations (4–13) constitute a set of equations of motion for atmospheric flight. Space flight can be described using the same equation set because aerodynamic force is substantially eliminated at high altitude due to the exponentially decreasing atmospheric density. However, at high altitude, it is numerically difficult to determine the control variables because the aerodynamic force is too small to contribute to the optimal trajectory. Therefore, the control variables are eliminated at high altitude through the following constraints:

$$C_L \cdot (h - h_{\text{atmos}}) \leq 0 \tag{14}$$

$$\sigma^2 \cdot (h - h_{\text{atmos}}) \leq 0 \tag{15}$$

where h_{atmos} is a maximum altitude at which aerodynamic control forces are assumed effective.

In addition to path constraints (14) and (15), several path constraints are introduced during space and atmospheric flight. One constraint is a minimum-altitude constraint, $h \geq h_{\min}$. Another constraint is an aerodynamic heating constraint. Hypersonic atmospheric flight causes high aerodynamic heating on the AOTV. Thus, it is necessary that the aerodynamic heating of the AOTV be constrained. In this study, an aerodynamic heating rate is used as an index to evaluate the aerodynamic heating. On the basis of the modified Chapman equation, the heating-rate constraint[11,15] becomes

$$Q_{\max} \geq Q = K_Q\sqrt{\rho/\rho_s}(v/v_s)^{3.15} \tag{16}$$

where K_Q is the aerodynamic heating-rate coefficient, the subscript s refers to sea level values, and v_s is circular orbit velocity at sea level.

Target Interception

The target intercepted by the AOTV is assumed to be located on a circular orbit. This orbit can be described by radius r_t, inclination i, longitude of the ascending node Ω, initial argument of latitude at epoch θ_{t0}, and time t, as shown in Fig. 1.

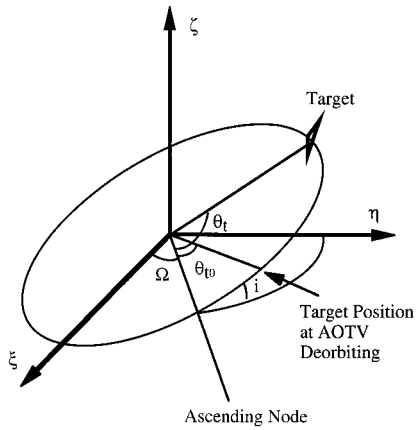

Fig. 1 Coordinate system for target motion.

In the target orbit plane, the angle from ascending node to the target may be expressed as

$$\theta_t = \theta_{t0} + \omega \cdot t \tag{17}$$

where

$$\omega = (1/r_t)\sqrt{\mu/r_t} \tag{18}$$

The position of the target may be expressed in Cartesian coordinates in the space-fixed frame as

$$\begin{pmatrix} \xi_{\text{tar}} \\ \eta_{\text{tar}} \\ \zeta_{\text{tar}} \end{pmatrix} = \begin{pmatrix} \cos\Omega & -\sin\Omega & 0 \\ \sin\Omega & \cos\Omega & 0 \\ 0 & 0 & 1 \end{pmatrix} \begin{pmatrix} 1 & 0 & 0 \\ 0 & \cos i & -\sin i \\ 0 & \sin i & \cos i \end{pmatrix} \begin{pmatrix} \cos\theta \\ \sin\theta \\ 0 \end{pmatrix} \tag{19}$$

The interception condition is that the target has the same position as the AOTV at the final time. This requires

$$\xi_{\text{tar}} = \xi_{\text{AOTV}} = (r_e + h) \cdot \cos\phi \cdot \cos\theta \tag{20}$$

$$\eta_{\text{tar}} = \eta_{\text{AOTV}} = (r_e + h) \cdot \cos\phi \cdot \sin\theta \tag{21}$$

$$\zeta_{\text{tar}} = \zeta_{\text{AOTV}} = (r_e + h) \cdot \sin\phi \tag{22}$$

Flight-Path Optimization

To find the flight path for minimum-time AOTV interception, the problem is formulated as an optimal control problem, i.e., a problem of finding state and control variable time histories to minimize a cost function for a system. The system is described by equations of motion, initial and terminal conditions, and might include other algebraic constraints such as path constraints, i.e., we wish to find

$$\min J[\boldsymbol{x}(t), \boldsymbol{u}(t), T] \tag{23}$$

subject to

$$\dot{\boldsymbol{x}}(t) = \boldsymbol{f}[\boldsymbol{x}(t), \boldsymbol{u}(t)] \tag{24}$$

$$\boldsymbol{x}(0) = \boldsymbol{x}_0 \tag{25}$$

$$\boldsymbol{x}(T) = \boldsymbol{x}_f \tag{26}$$

$$\boldsymbol{g}[\boldsymbol{x}(t), \boldsymbol{u}(t)] \leq \boldsymbol{0} \tag{27}$$

where $\boldsymbol{x}(t)$ is the vector of state variables, $\boldsymbol{u}(t)$ is the vector of control variables, T is the final time, and $\boldsymbol{g}[\boldsymbol{x}(t), \boldsymbol{u}(t)]$ is a vector of state variable inequality constraints.

The optimal control problem [Eqs. (23–27)] is converted to a nonlinear programming problem (NLP) using a form of the DCNLP method. This method has been chosen because of its robustness and adaptability. DCNLP converts an optimal control problem into an NLP through the following process.

1) Divide the time history of the problem into segments (usually of equal length).

2) Approximate the solution of the equations of motion on each segment as a polynomial and describe the system by algebraic system constraints.

3) Discretize all state and control variables and collect them as a set of parameters.

4) Find the set of parameters that minimizes the cost function under the algebraic constraints, i.e., solve the resulting NLP problem.

There are several forms of the DCNLP method to choose from.[2–5] The principal difference between these methods is how the second step of the process just described is accomplished, i.e., how the state variable time history is modeled. The method chosen for this work is based on assuming a fifth-degree polynomial for the state history and is equivalent to integration using a fifth-degree Gauss–Lobatto quadrature rule; it is completely described in previous papers.[4,5]

The routine NZSOL[16] is used as the NLP solver. For efficiency, an analytical Jacobian is used, and the problem variables are scaled, i.e., the parameter vector of the solution contains numbers of approximately the same order of magnitude. The length, time, and mass scaling units chosen are equivalent to 1.1126×10^6 m, 14.067 s, and 4842 kg, respectively. As heating rate cannot be properly scaled by a normalizing unit, an additional scaling factor is set for the nondimensional heating rate. After scaling, K_Q becomes 22.857. The dimensional and scaled value of AOTV orbit, vehicle data, and required physical constants are shown in Table 1. All scaled values are expressed using upper bars.

Table 1 Mission data, AOTV data, and physical constants

Quantities	Dimensional value	Scaled value
v_{s0}	7.6676e+3, m/s	9.6951e−0
h_0	4.0744e+5 m	3.6623e+0
θ_0	0.0000e+0, rad	0.0000e+0
ϕ_0	0.0000e+0, rad	0.0000e+0
r_t	6.4897e+6, m	5.8333e+1
Ω	0.0000e+0, rad	0.0000e+0
θ_{t0}	0.0000e+0, rad	0.0000e+0
C_{D0}	3.2000e−2	3.2000e−2
K	1.4000e+0	1.4000e+0
m	4.8420e+3, kg	1.0000e+1
S	1.1690e+1, m^2	9.4457e−10
h_{atmos}	1.5575e+5, m	1.4000e+0
$h_{\min}$	0.0000e+0, m	0.0000e+0
r_e	6.3784e+6, m	5.7333e+1
v_s	7.9087e+3, m/s	1.0000e+0
β	7.3575e+3, m	6.6134e−2
μ	3.9860e+14, m^3/s^2	5.7333e+1
ρ_s	1.0782e+0, kg/m^3	5.7785e+16

Suitability of DCNLP for AOTV Trajectory Optimization

Before proceeding with the optimal interception problem, we will first evaluate the suitability of the DCNLP method for AOTV trajectory optimization. Minimum-energy-loss, i.e., maximum final velocity, orbit transfer trajectories for an AOTV have been found using the high-resolution DCNLP method and are compared with trajectories found recently by Seywald[10] using a shooting method. To make an accurate comparison, essentially the same equations of motion and heating-rate constraints employed by Seywald[10] are used, i.e., the equations of motion consist of Eqs. (4–13) and the heating-rate constraint is described by Eq. (16). Instead of initial condition [Eq. (3)] and terminal conditions [Eqs. (17–22)], the trajectory of the AOTV starts at altitude 111.3 km (=60 n mile and scaled altitude = 1.0) with velocity 7847 m/s (scaled velocity = 0.9922) and flight-path angle -9.599×10^{-3} rad (=−0.55 deg) and terminates at the same altitude as the initial altitude after penetration of the atmosphere. The cost function (to be maximized) for the minimum-energy-loss trajectory is the final velocity of the AOTV.

Table 2 Comparison of result between DCNLP and shooting method

Heating-rate constraint, Btu/ft^{2}s	DCNLP (this research)		Shooting method (Seywald[10])	
	Final time, s	Final velocity, m/s	Final time, s	Final velocity, m/s
771.676 (unconstrained)	1005.059	6718.697	1005.877	6718.864
700	1022.446	6715.613	1034.706	6714.103
600	1046.894	6688.565	1082.117	6688.533
500	1074.874	6626.402	N/A	N/A
400	1083.497	6485.152	N/A	N/A
350	1096.691	6311.477	N/A	N/A

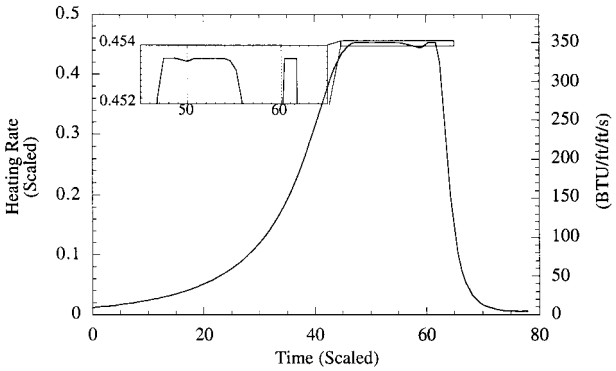

Fig. 2 Heating-rate history for minimum-energy loss AOT; Q_{max} = 350 Btu/ft^{2}s.

The problem is successfully solved for several different heating-rate constraints. Some characteristics of the result using DCNLP and using a shooting method are shown in Table 2. Table 2 shows that the result using DCNLP corresponds well to the result using a shooting method[10] in the case of inactive heating-rate constraint, i.e., 6718.697 m/s vs 6718.864 m/s. Even if the heating-rate constraint is active somewhere on the trajectory, the final velocity found using DCNLP is almost the same as that using a shooting method. The difference in final time between the DCNLP solution and a shooting solution increases as the heating-rate constraint decreases. However, the difference is still only several percent even in the case of $Q_{max} = 600$ Btu/ft^{2}s.

Another interesting result is that DCNLP can solve the problem with a very restrictive heating-rate constraint. Seywald[10] stated that he tried to solve it using a direct method but could not. He also predicted that the solution includes "at least three constrained arcs" under heating-rate constraint less than 450 Btu/ft^{2}s, on the basis of several numerical experiments. The DCNLP solution identifies three constraint arcs on the optimal solution for $Q_{max} = 350$ Btu/ft^{2}s, as shown in Fig. 2. (However for $Q_{max} = 400$ Btu/ft^{2}s, only two constraint arcs are identified.) Thus, it appears that DCNLP is a suitable, robust solution method for the AOTV trajectory optimization problem.

Minimum-Time AOTV Interception

While any initial orbit could be chosen for each of the two vehicles, the AOTV is assumed to be in a circular orbit at altitude 407.4 km (=220 n mile) until deorbiting, the same initial orbit chosen in the work of Andrews et al.[17] The maximum allowable initial impulse is assumed to be 790.9 m/s. The target is located on a circular orbit at altitude 111.3 km (=60 n mile). The initial conditions for the AOTV orbit are shown in Table 1. Most of these data are based on those used by Seywald.[10] Minimum allowable flight altitude is set to 0, and the maximum altitude at which aerodynamic control is effective is assumed to be 155 km. In the discretization of the problem, 20 segments are used.

Two surveys are done in this section. In the first survey, the target inclination is varied between 0.06 and 0.4 rad. Inasmuch as one of the established advantages of AOT is to generate forces for out-of-plane motion, optimal trajectories requiring orbital plane change are expected to show the use of AOT. Also, minimum-time interception by ballistic flight, which means $C_L = 0$ during all flight phases, is solved under the same conditions for comparison.

A second survey is done for minimum-time AOT interception under heating-rate constraint. The cases are solved with between 0.07 and 0.1 rad of target inclination under the heating-rate constraint $\bar{Q}_{max} = 0.7$. It is expected that a comparison between the case of $\bar{Q}_{max}$ free and the case of $\bar{Q}_{max} = 0.7$ will show an effect of aerodynamic heating constraint on minimum-time AOT interception.

Optimal trajectories for minimum-time AOT interception have been found for target inclinations of $i = 0.06$, 0.08, 0.1, 0.2, 0.3, and 0.4 rad. The time histories of altitude and velocity of the AOTV are shown in Figs. 3 and 4, respectively. Time histories of the control variables, the lift coefficient and bank angle, are shown in Figs. 5 and 6. The heating-rate history for each of these optimal trajectories is shown in Fig. 7. In addition to these cases using AOT, optimal ballistic flight cases for target inclinations $i = 0.06$, 0.08, and 0.085 rad have been found. From the solutions, four basic observations have been made.

1) A minimum-time AOT interception trajectory at $i = 0.06$ rad is almost the same as the ballistic flight interception trajectory.

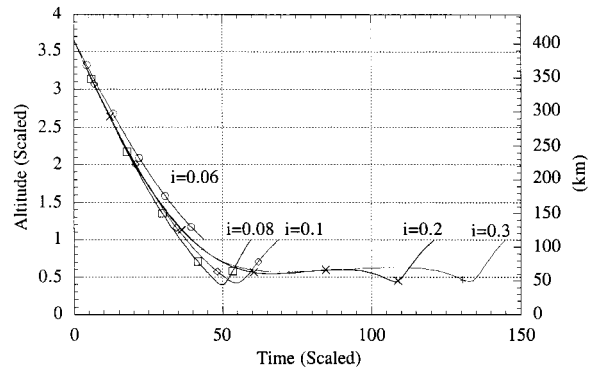

Fig. 3 Altitude history for minimum-time AOT interception; no heating-rate constraint.

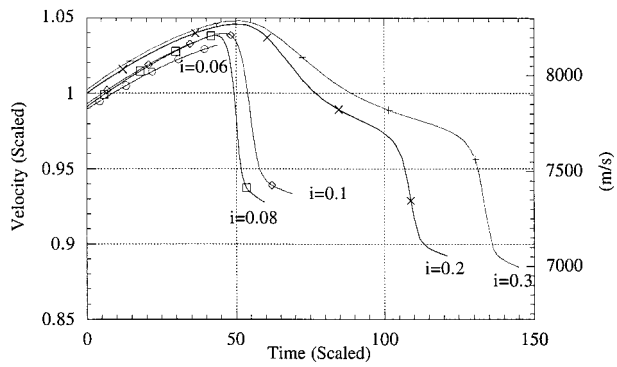

Fig. 4 Velocity history for minimum-time AOT interception; no heating-rate constraint.

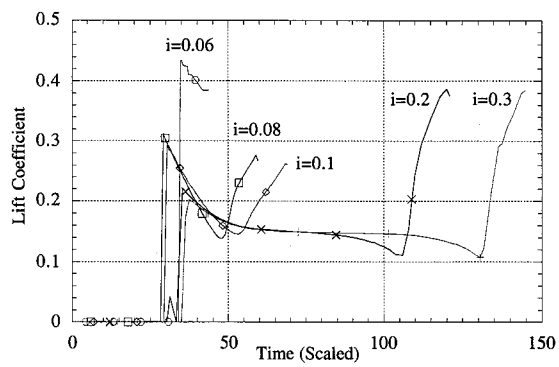

Fig. 5 Lift coefficient history for minimum-time AOT interception; no heating-rate constraint.

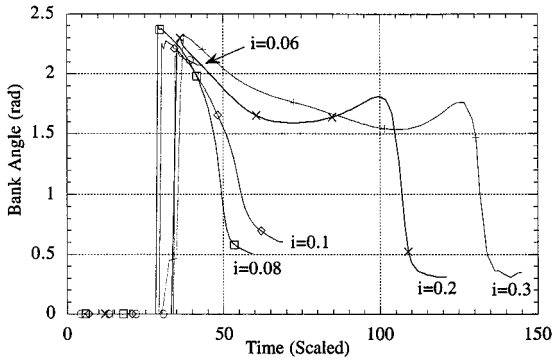

Fig. 6 Bank angle history for minimum-time AOT interception; no heating-rate constraint.

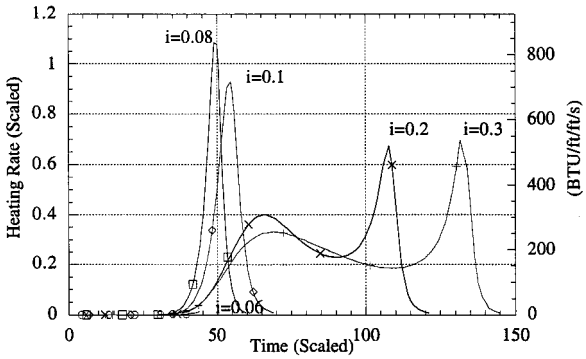

Fig. 7 Heating-rate history for minimum-time AOT interception; no heating-rate constraint.

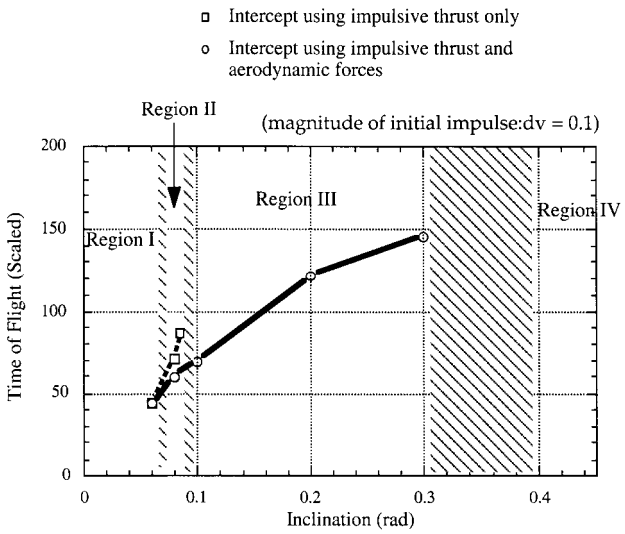

Fig. 8 Target interception time vs target orbit inclination wherein region I minimum-time interception is accomplished using initial impulse only; region II minimum-time interception is accomplished by AOT combined with initial impulse, interception by initial impulse only is feasible; region III minimum-time interception is accomplished by AOT combined with initial impulse, interception by initial impulse only is not feasible; and region IV interception is not feasible.

2) A minimum-time interception at $i = 0.08$ rad is done using AOT. A ballistic flight can intercept the target but needs a longer flight time than when AOT is used.

3) Minimum-time interceptions at $i = 0.1$, 0.2, and 0.3 rad are done using AOT. For these inclinations, a purely ballistic flight trajectory cannot intercept the target.

4) At $i = 0.4$ rad, there is no interception trajectory.

Figure 8 shows these four types of trajectories corresponding to four ranges of target inclination. Trajectories using AOT have a longer flight path than ballistic flight because AOT requires that the vehicle go down into dense regions of the atmosphere. Therefore, in the case of small change of orbital plane, AOT has a disadvantage for time of flight due to the longer flight path. This is shown as region I in Fig. 8. On the other hand, AOT may reduce the time of flight because the AOTV can improve the transfer trajectory using fuel at the initial impulse that the ballistic vehicle requires for plane change (but that the AOTV accomplishes in part using aerodynamic forces). Region II shows the range of target inclination such that the advantage of fuel saving due to use of AOT outweighs the disadvantage due to lengthened flight path. If an initial impulse cannot establish a velocity vector required for interception, ballistic flight is not feasible. AOT is indispensable for change of orbital plane in region III. Region IV shows the target inclinations such that AOTV cannot intercept the target even if AOT is used. The results show that AOT trajectories may yield minimum-time interception, even if ballistic flight alone can intercept the target.

Aerodynamic force is significantly used for trajectories that pass below $\bar{h} = 0.6$ (=66.8 km). This is deduced from the result that significant heading angle change occurs under this altitude in every AOT case. The interception trajectories at $i = 0.2$ and 0.3 rad in Fig. 3 are most interesting. These show the AOTV flies a nearly constant altitude around $\bar{h} = 0.6$ during the intermediate flight phase. Inasmuch as an AOTV can significantly control flight path under this altitude, an AOTV needs to stay at most around $\bar{h} = 0.6$ immediately before target interception.

The maximum C_L used is around 0.4, which occurs at approximately 40 deg of angle of attack.[18] Also, during constant altitude flight for $i = 0.2$ and 0.3 rad, C_L assumes a value to maximize L/D. This is characteristic of optimal aeroassisted orbital transfer trajectories.[10,14]

For minimum-time AOT interception, the case of maximum aerodynamic heating rate $\bar{Q}_{\max}$ free and the case of $\bar{Q}_{\max} = 0.7$ are compared at target inclinations $i = 0.08$ and 0.1 rad. From Fig. 7, one can see that these are the only cases where this constraint will be effective. The AOTV velocity time histories for the constrained and unconstrained cases for target inclination $i = 0.08$ rad are compared in Fig. 9. The interception under $\bar{Q}_{\max} = 0.7$ needs 61.2 time units, and the interception under $\bar{Q}_{\max}$ free needs 59.4. The effect of heating-rate constraint on time of flight is not large. An increase in the time of flight due to heating-rate constraint is around only 3% at $i = 0.08$ rad. An increase in the time of flight at $i = 0.1$ rad, 1%, is smaller than the increase at $i = 0.08$ rad. The maximum aerodynamic heating constraint significantly affects the time histories of the controls, the lift coefficient (Fig. 10), and the bank angle.

The initial heading angle chosen by the optimizer under $\bar{Q}_{\max}$ free is smaller than that under $\bar{Q}_{\max} = 0.7$. To reduce aerodynamic heating for the AOTV, the AOTV flies higher. However, the direction of the initial impulse vector is changed to increase initial heading angle to supplement the reduced rate of heading angle change because of low atmospheric density. Therefore, the AOTV subject to heating-rate constraint can intercept the target without a large delay. The maximum heating rate can thus be relaxed by a small extension of time of flight. Time of flight can be used as a tradeoff parameter for reduction of aerodynamic heating without a large penalty.

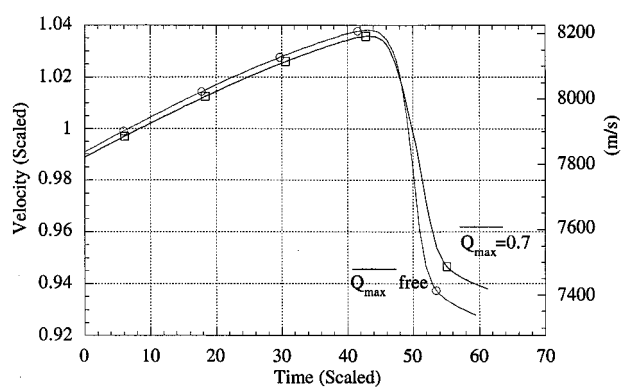

Fig. 9 Velocity history for minimum-time AOT interception; heating-rate constraint.

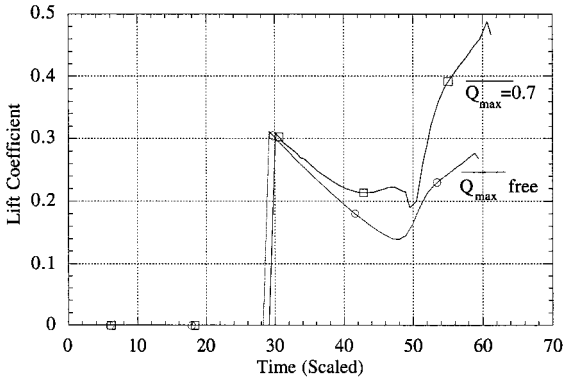

Fig. 10 Lift coefficient history for minimum-time AOT interception; heating-rate constraint.

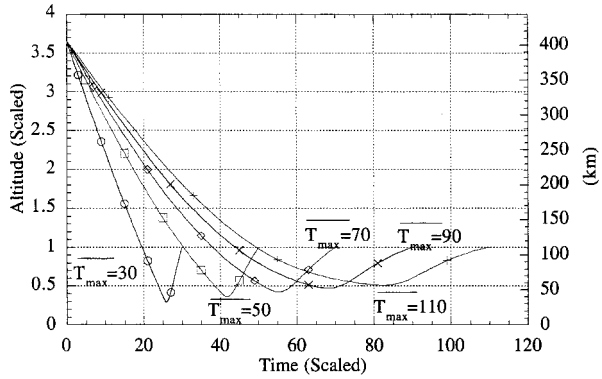

Fig. 11 Altitude history for minimum-fuel AOT interception; no heating-rate constraint.

Minimum-Fuel AOT Interception

Minimum-fuel AOT interception has also been studied. Because only one impulse is allowed, minimizing the magnitude of the impulse, or equivalently but more easily, the square of the magnitude of the initial impulse, yields the minimum-fuel trajectory. The mission data, AOTV data, and physical constants of Table 1 are used again. The characteristics of minimum-time interception will be compared with the results for minimum-fuel interception.

Target inclination is fixed to 0.1 rad, and the maximum allowable time of flight, T_{max}, has been fixed to avoid infinite times of flight. Scaled maximum allowable time of flight ranges from 30 to 110. Additionally, the effect of heating rate constraints has been studied by solving the case of $\bar{T}_{max} = 30.0$ under the constraint $\bar{Q}_{max} = 2.0$.

Cases of minimum-fuel interception have been solved for $\bar{T}_{max} = 30$, 50, 70, 90, and 110 time units. The altitude and velocity time histories for these cases are shown in Figs. 11 and 12, respectively. The heating-rate history for each trajectory is shown in Fig. 13. The required initial impulse magnitude vs maximum allowable time of flight is shown in Fig. 14. The shorter is the time of flight, the larger is the initial impulse required. The reason for this is that the AOTV needs a large heading angle change by the initial impulse so that the AOTV can intercept the target in a short time.

The velocity of the AOTV at the final time increases, for the minimum-fuel case, as allowed time of flight increases, as shown in Fig. 12. However, because the target velocity in its circular orbit is $v_{tar} = 0.988$, the relative velocity between the AOTV and the target at interception always decreases with increasing time of flight. Flight-path angle at interception is close to zero when the maximum allowable time of flight becomes large. This means that the AOTV intercepts the target near the apogee point of its postatmospheric-passage orbit, where its absolute velocity is minimized, when the time of flight increases. It is observed that a quite different result obtains for minimum-time interception; in this case the interception of the target occurs when the AOTV has a relatively high absolute velocity, i.e., away from orbit apogee.

The decrease in maximum allowable time of flight causes an increase in maximum heating rate, as shown in Fig. 13. The AOTV must fly into dense atmosphere to intercept the target by minimum fuel within a short time. As heating rate is proportional to the square root of atmospheric density, maximum heating rate increases for low-altitude flight. This observation, that extension of time of flight relaxes maximum heating rate, is the same found for minimum-time AOT interception.

The optimal minimum-fuel trajectory for the case of $\bar{T}_{max} = 30.0$ under the heating-rate constraint $\bar{Q}_{max} = 2.0$ has been determined. It can be seen from Fig. 13 that this constraint will be effective. Although the maximum heating rate decreases by 20% from that of the unconstrained case, the initial impulse shows only slight increase from 0.16664 to 0.16731. An increase in C_L reduces the amount of decrease seen in the heading angle due to high-altitude flight. Only a part of heading angle change that cannot be supplemented by this C_L increase is supplemented by an increase in initial impulse. This result suggests that constraints on maximum heating rate can largely be compensated for by a small increase in fuel use.

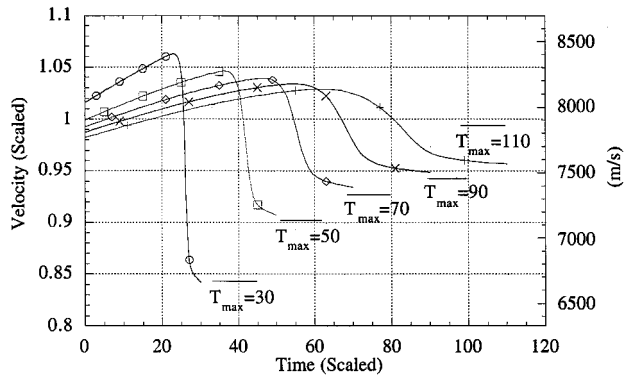

Fig. 12 Velocity history for minimum-fuel AOT interception; no heating-rate constraint.

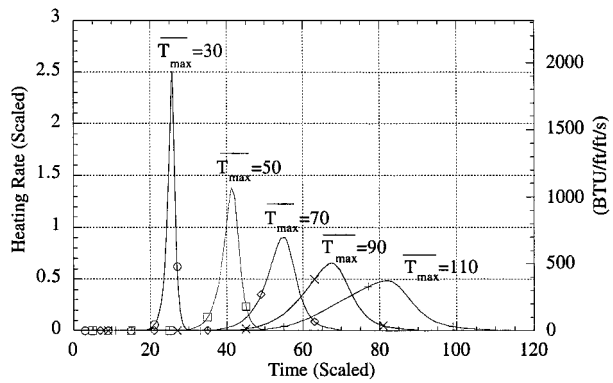

Fig. 13 Heating-rate history for minimum-fuel AOT interception; no heating-rate constraint.

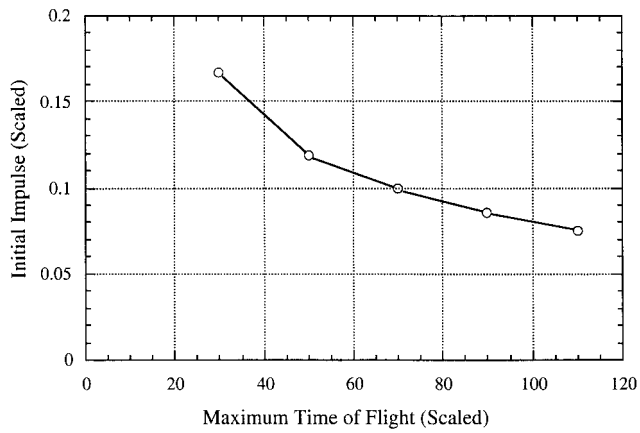

Fig. 14 Initial impulse magnitude for minimum-fuel interception vs time of flight.

Conclusions

The problem of minimum-time and minimum-fuel trajectory optimization for interception of an orbiting target by a vehicle using a propulsive maneuver followed by AOT has been solved for a range of different target orbit inclinations and interceptor vehicle heating-rate constraints.

A principal result is that four different regions of qualitatively different trajectories exist as a function of increasing target inclination. Remarkably, it is found that minimum-time interception may require the use of AOT even though it is possible to intercept a target by ballistic flight alone. Therefore, an AOTV has advantages for minimum-time target interception compared with ballistic flight. Time of flight increases under heating rate constraint. This increase is an order of only several percent compared with the no heating constraint case. Thus, by permitting a small increase of time of flight, the aerodynamic heating rate can be relaxed.

A second important result has to do with the suitability of the DCNLP method for the solution of this type of problem. This solution method proved to be robust and efficient and very simply allows the incorporation of constraints on the states or the controls. It is able to solve difficult cases including multiple constrained arcs.

In future research on this subject it would be wise to remove the simplification of a nonrotating atmosphere and use a more sophisticated atmospheric density model. There is no limit to the number of possible initial conditions of orbits for both target and interceptor vehicle, as well as initial relative position; only a few have been considered here and so a wider range for these parameters might be considered in future work.

References

[1]Bryson, A. E., and Ho, Y. C., *Applied Optimal Control*, Hemisphere, New York, 1975, Chap. 3.

[2]Hargraves, C. R., and Paris, S. W., "Direct Trajectory Optimization Using Nonlinear Programming and Collocation," *Journal of Guidance, Control, and Dynamics*, Vol. 10, No. 4, 1987, pp. 338–342.

[3]Enright, P. J., and Conway, B. A., "Optimal Finite-Thrust Spacecraft Trajectories Using Collocation and Nonlinear Programming," *Journal of Guidance, Control, and Dynamics*, Vol. 14, No. 5, 1991, pp. 981–985.

[4]Herman, A. L., "Improved Collocation Methods with Application to Direct Trajectory Optimization," Ph.D. Dissertation, Dept. of Aeronautical and Astronautical Engineering, Univ. of Illinois, Urbana–Champaign, IL, 1995.

[5]Herman, A. L., and Conway, B. A., "Direct Optimization Using Collocation Based on High-Order Gauss–Lobatto Quadrature Rules," *Journal of Guidance, Control, and Dynamics*, Vol. 19, No. 3, 1996, pp. 592–599.

[6]Miele, A., Basapur, V. K., and Lee, W. Y., "Optimal Trajectory for Aeroassisted Noncoplanar Orbital Transfer," *Acta Astronautica*, Vol. 15, No. 6/7, 1987, pp. 399–411.

[7]Miele, A., "Recent Advances in the Optimization and Guidance of Aeroassisted Orbital Transfers," *Acta Astronautica*, Vol. 38, No. 10, 1996, pp. 747–768.

[8]Medepalli, S., and Vinh, N. X., "Optimal Plane Change of an Elliptic Orbit During Aerocruise," *Journal of Astronautical Sciences*, Vol. 40, No. 4, 1992, pp. 503–525.

[9]Naidu, D. S., *Aeroassisted Orbital Transfer Guidance and Control Strategy*, Springer–Verlag, New York, 1994, Chaps. 4 and 5.

[10]Seywald, H., "Variational Solution for the Heat-Rate-Limited Aeroassisted Orbital Transfer Problem," *Journal of Guidance, Control, and Dynamics*, Vol. 19, No. 3, 1996, pp. 686–692.

[11]Lee, J. Y., and Hull, D. G., "Maximum Orbit Plane Change with Heat-Transfer-Rate Considerations," *Journal of Guidance, Control, and Dynamics*, Vol. 13, No. 3, 1990, pp. 492–497.

[12]Prussing, J. E., and Conway, B. A., *Orbital Mechanics*, Oxford Univ. Press, New York, 1993, Chap. 6.

[13]Vinh, N. X., Busemann, A., and Culp, R. D., *Hypersonic and Planetary Entry Flight Mechanics*, Univ. of Michigan Press, Ann Arbor, MI, 1980, Chap. 2.

[14]Hull, D. G., Giltner, J. M., Speyer, J. L., and Mapar, J., "Minimum Energy-Loss Guidance for Aeroassisted Orbital Plane Change," *Journal of Guidance, Control, and Dynamics*, Vol. 8, No. 4, 1985, pp. 487–493.

[15]Chapman, D. R., "An Approximate Analytical Method for Studying Entry into Planetary Atmospheres," NASA TR R-11, 1959.

[16]Gill, P. E., Saunders, M. A., and Murray, W., "User's Guide for NZOPT 1.0: A Fortran Package for Nonlinear Programming," McDonnell Douglas Aerospace, Huntington Beach, CA, 1993.

[17]Andrews, D. G., Norris, R. B., and Paris, S. W., "Benefits of High Aerodynamic Efficiency to Orbital Transfer Vehicles," AIAA Paper 83-2109, Aug. 1983.

[18]Zimmermann, F., and Calise, A. J., "Aeroassisted Orbital Transfer Trajectory Optimization Using Direct Methods," AIAA Paper 95-3478, Aug. 1995.